PEER-REVIEWED ARTICLE

Scale-Dependent Errors in the Estimation of Land-Cover Proportions: Implications for Global Land-Cover Datasets

Aaron Moody and Curtis E. Woodcock

Abstract

Aggregation of fine-resolution land-cover maps to coarser scales indicates that estimates of the proportions of land-cover types vary as a function of spatial resolution. The magnitude of these proportional errors in a forested area in northern California increase significantly as resolution exceeds a 90-m threshold. These errors could pose difficulties for the use of land-cover products generated from coarse-resolution sensors such as the NOAA-AVHRR and the MODIS sensor planned for the EOS program. The magnitude of the errors appears to be a function of the spatial resolution of the map, the original size of the land-cover classes, and the spatial patterns of the classes.

Introduction

Physical and ecological phenomena at a broad range of scales are inherently linked to the composition, extent, and structure of the land cover. Moreover, transformations in the composition and distribution of land cover represent one of the most dramatic sources of systematic change at local, regional, and global scales. These changes carry with them tremendous implications for climates, biogeochemical processes, surface processes, and ecosystems. Surface characteristics, including land cover, affect many processes such as momentum transfer, water cycling, absorption of solar radiation, emission of thermal radiation, carbon cycling, and latent and sensible heat fluxes. Changes in land cover, as well as those processes which are influenced by these changes, can impact biological productivity, stability, and diversity at a broad range of scales (Townshend *et al.*, 1993). Because of these relationships, research such as local studies of ecosystem dynamics and biological diversity; regional analysis of hydrologic processes; and global models of climate and biogeochemical cycles all must incorporate the influence of land cover on the phenomena of interest. For this to occur, some knowledge or representation of the land cover must be available in digital or analog form.

It is assumed that a high premium is placed on the accuracy of such land-cover datasets. However, accuracy, or even the land-cover units themselves, may not be defined in the same manner or hold the same importance when considered at different scales. To better understand the scaling issues and implications of accuracy in land-cover data, it is of interest to investigate the relationships between land-cover map error, scale of observation, and scene spatial structure. In this paper we attempt to develop an initial understanding of the ways in which the size and spatial pattern of vegetation classes in our Sierra Nevada test site influenced errors in estimating cover type proportions as the classified scene was progressively aggregated to coarser resolutions.

Continental or global scale land-cover datasets are perhaps the most problematic in terms of production, definition of cover types, and maintenance of acceptable levels of accuracy. While this research may have implications at a variety of scales, it is this issue of large area land-cover characterization which provides the primary context.

Small-Scale Land-Cover Databases

Numerous global-scale digital land-cover datasets have been developed for the purpose of supporting climate and biogeochemical cycle (BGC) models. These datasets are often used to provide spatial data on climatically or biophysically relevant surface parameters such as leaf area index (LAI), evapotranspiration (ET), and absorbed photosynthetically available radiation (APAR) (Wilson and Henderson-Sellers, 1985; Mathews, 1983; Olson and Watts, 1982). Such global vegetation maps have typically been collated from numerous preexisting sources and have not been subjected to any consistent level of ground validation or accuracy assessment (Wilson and Henderson-Sellers, 1985). They may also contain errors which result from faulty or outdated source data, difficulty in translating the categories in the source data to the desired map categories, and poor representation of agricultural areas and disturbed regimes (Townshend *et al.*, 1991).

Almost without exception, efforts to produce coarse resolution, large-area land-cover products using satellite data have involved the conversion of AVHRR (Advanced Very High Resolution Radiometer) bands one and two to the NDVI (Normalized Difference Vegetation Index). Land cover is then characterized based on the temporal signals of this indicator (Tucker *et al.*, 1985; Townshend *et al.*, 1987; Loveland *et al.*, 1991). These datasets suffer from technical limitations of the instrument such as poor pointing accuracy, poor calibration, and non-optimized band specifications. They are also limited by a lack of adequate pre-processing procedures such as atmospheric correction, cloud screening, and image-to-image

---

Center for Remote Sensing and Department of Geography, Boston University, 725 Commonwealth Avenue, Boston, MA 02215.

Photogrammetric Engineering & Remote Sensing,
Vol. 60, No. 5, May 1994, pp. 585–594.

0099-1112/94/6001–585$03.00/0

registration; and by insufficient resources for adequate ground-based validation efforts. While these datasets represent the heredity of future efforts to monitor and assess land cover at small scales, they may have reached the threshold of their utility due to the above limitations. As researchers in an increasing range of disciplines extend their analyses beyond local and regional scales, and as the land surface components of small-scale models evolve in terms of their complexity and sensitivity to inputs, the accuracy of new land-cover datasets deserves attention and should be carefully characterized in order to maximize the utility and scale flexibility of such products.

In the context of NASA's role in supporting the global science community through the Earth Observing System (EOS), the Land Group of the Moderate Resolution Imaging Spectroradiometer (MODIS) Science Team is developing algorithms for the production of a global land-cover dataset to be generated on a periodic basis using the low spatial resolution, high temporal frequency observations from the MODIS instrument (Running *et al.*, 1993). MODIS is scheduled for launch aboard the EOS-AM platform in June 1998, and is planned as the primary EOS instrument for large-scale monitoring of terrestrial and oceanic processes and dynamics. This sensor has 36 spectral bands in the range of 0.4 to 14 µm, with 250-m spatial resolution in the red and near infrared channels, 500-m resolution in the five visible and near infrared channels, and 1000-m resolution in the remaining bands (Running *et al.*, 1993). The land-cover product is planned as a 1-km data set produced on a quarterly basis. This spatial resolution is appropriate for regional scale climate and surface process models, but will need to be aggregated to coarser scales to support continental or global scale modeling efforts.

Two issues arise, then, as the definition and algorithm development activities proceed for this and other global land- cover datasets. While global-scale models which incorporate sub-grid scale processes will probably not be sensitive to the locational accuracy of spatially varying input parameters at the sub-grid scale, they will be sensitive to the proportional representation of these component inputs within the cell. This leads us first to question whether the representation of the landscape at 1-km resolution, as derived from 250-m, 500-m, and 1-km data, adequately maintains the proportional accuracy of the component cover types in the scene. Second, if the development of new global datasets is to represent an improvement over previously existing products, then considerable effort must be devoted to the validation and accuracy assessment of these datasets. This raises the difficult issue of using high resolution land-cover information from local maps and/or from remotely sensed sources to assess the quality of coarse resolution characterizations of land cover. Finally, can a reasonable level of proportional accuracy be maintained when 1-km land-surface data are aggregated to the grid-cell size of global scale models? This paper focuses primarily on the first of these three questions, with implications for the latter two.

Background

Davis *et al.* (1991) reviewed many of the basic issues relating to the scale dependence of geographic data. This was primarily in the context of identifying, characterizing, and modeling scales of spatial dependence and variability, with the aim of developing theory to aid in the sampling of spatial data and the integration of spatial databases. Within the context of this large and complex set of problems, numerous researchers in the remote sensing community have investigated the influence of spatial resolution on the accuracy of land-cover mapping. These efforts have involved assessing the characteristics of several representations of a given area, either sampled at different resolutions by different sensors, or aggregated to a series of coarser scales from a single high-resolution dataset. Latty and Hoffer (1981) degraded Thematic Mapper Simulator data to a series of coarser resolutions and compared the results of a maximum-likelihood classification of the scene at the different scales. These authors noted an improvement in classification accuracy as the data were coarsened within the range of 15 m to about 75 m resolution. Sadowski *et al.* (1977) found the same phenomenon for forested landscapes using degraded aircraft Multispectral Scanner (MSS) data. They noted that the improvement of classification accuracy at coarser resolutions was related to the inherent scale associated with the classification scheme employed. Markham and Townshend (1980) produced a similar analysis and discussed a complex set of processes whereby changes in classification accuracy with coarsening resolution depended on class-specific variances and covariances, the location of cover-type units relative to the overall scene, and mixed pixels at class boundaries which lead to classification errors. Cushnie (1987) found similar results in her assessment of within-class variability as a function of spatial resolution and the implications for land-cover classification. The works cited above investigated the effect of resolution on classification performance for a series of resolutions which were all finer than the fundamental resolution of the defined cover-type units. In this context, improved classification performance at coarser resolutions was largely a response to a reduction in within-class variability inherent in the process of averaging signals over larger areas (Sadowski *et al.*, 1977). In their comparison of land-cover classification accuracies for Landsat MSS and AVHRR data, Gervin *et al.* (1985) found that, while overall AVHRR accuracy was nearly as good as MSS for very broad land-cover categories, performance varied considerably between study sites and for different cover types. Their discussion attributed these inconsistencies to the interrelationship between the scale of observation, the dominance of individual cover types at the different study areas, and the spatial pattern of the land-cover classes.

Other work has focused on the relationship between sampling resolution and the spatial properties of the scene. Woodcock and Strahler (1987) assessed the relationship between resolution and local variance for a variety of cover types as well as for simulated scenes. They discussed their results, in part, in terms of the effect of the interaction between spatial resolution and scene structure on mapping accuracy. In general, the local variance was found to be a function of the relationship between the size of scene objects and the sampling resolution. Townshend and Justice (1988) used a similar approach to investigate the relationship between spatial resolution and the ability to assess land surface changes at the global scale. They degraded MSS data to a series of coarser resolutions between 250 and 4000 m, generated difference images from multi-date image pairs at given resolutions, and performed numerous analyses investigating changes in image properties as resolution was degraded. These observations included dramatic changes in the proportions of test site images falling within specific NDVI ranges as the scenes were progressively degraded to coarser resolutions. They noted that, at 1 km resolution, large-area land-surface changes can be identified but not quantified. Townshend and Justice (1990) also noted that one difficulty in determining an appropriate sampling resolution stems from the fact that the scene variance is composed of contributing variances at a wide range of scales.

The literature in landscape ecology has, in recent years, displayed an increasing focus on issues related to the scale dependence of ecological phenomena (Turner *et al.*, 1989b). This work has included investigations into the importance of scale in understanding landscape disturbance and ecosystem dynamics, as well as the need to address scaling issues when characterizing landscape heterogeneity and diversity (Meentmeyer and Box, 1987; Turner *et al.*, 1989a). Investigations into the links between the scale of observation, landscape patterns, and land-cover proportions have evolved out of the importance of these relationships for understanding ecological processes (Turner *et al.*, 1991). Scaling issues have become especially important in this field as researchers attempt to extend investigations from local to regional scales, requiring the comparison, extrapolation, and integration of data across spatial scales (Meentmeyer and Box, 1987; Turner *et al.*, 1989b).

Turner *et al.* (1989a) investigated the effect of changing map scales on apparent landscape pattern and attempted to relate some simple measures of landscape diversity, dominance, and contagion to the observed changes in spatial pattern. Using existing land-cover maps, they found rates of loss or increase in cover-type proportions with changing scale of observation to be related to spatial pattern (contagion) as well as original class proportions (dominance). These authors wrote of the need for methods to either mitigate the loss of information due to the transference of phenomena across measurement or analysis scales, or to quantify the reduced information content. Some of the primary issues involved in the transference of information across scales include the identification of critical scaling thresholds across which extrapolation is not feasible, understanding the relationship between scale dependent variance and such thresholds, and understanding the degree to which translation between fine and coarse scales is direction dependent (Rosen, 1989; Turner *et al.*, 1989b).

The purpose of this paper is to continue the study of proportional errors as they relate to scale, or spatial resolution. However, rather than begin with a land-cover map that already includes some degree of generalization, we used data derived directly from 30-m TM imagery. This paper focuses on these issues in terms of assessing land cover at a wide range of scales using remotely sensed data, and the subsequent use or further aggregation of these datasets. Results are discussed with specific reference to the spatial characteristics of the cover types in the study area, and an initial attempt is made to generalize these relationships.

Methods

This research employs data from the western part of the Plumas National Forest in the northern Sierra Nevada in California. The Plumas site has been studied recently as part of a project to develop land-cover mapping and timber-inventory methods for the U.S. Forest Service (Woodcock *et al.*, 1993). Land-cover maps for the site were produced using Landsat Thematic Mapper imagery and unsupervised image classification procedures supported by air-photo and field validation. The general cover classes for this dataset include *barren/grass, brush, hardwood, meadow, conifer,* and *water.* Meadows are omitted from this study due to their small size and relative infrequency.

For this research, the 30-m resolution per-pixel land-cover map of the Plumas National Forest study area was used as the baseline data (Plate 1). This map was used to label a series of coarser resolution maps of the scene which were produced through an aggregation procedure described below. The resulting dataset allowed the examination of changes in land-cover proportions as a function of the scale of observation. Resolutions considered were 30, 90, 150, 240, 510, 1020, 3000, and 6000 metres. The 240-, 510-, and 1020-m resolutions roughly coincide with the spatial resolutions of MODIS.

Polygon grids were generated to serve as sampling frames for each of the resolutions of interest. For example, the polygons for the 90-m aggregation grid each contained nine 30-m pixels. These were overlayed on the per-pixel class map and each grid cell or polygon was labeled based on the most frequently occurring cover type among the high resolution pixels within that polygon. This procedure was performed for each of the aggregation levels. After this plurality based resampling, the percentage of each cover type within each of the coarser resolution class maps was calculated and normalized by the percentage of pixels considered to be outside the study area for that particular resampling scale. In this way, the classified portion of each dataset was normalized to 100 percent of the total area considered.

Clearly, this procedure does not replicate the direct classification of remotely sensed data at a series of image resolutions. Rather, the purpose of this study was to investigate the proportional error due to spatial mixing of cover types under the simplest of conditions; that is, where errors in cover-type estimation relate only to spatial aggregation toward coarser scales and are not further convolved by sensor response characteristics, atmospheric effects, or spectral mixing of scene elements. For this reason, aggregation was performed on the high-resolution class map and not on the original imagery used for the classification. The per-pixel land-cover map was used as the reference against which the coarser resolution maps were compared. The accuracy of this map has been assessed using methods based on fuzzy sets (Gopal and Woodcock, 1994). Using a stringent MAX operator, the general land-cover classes are 84% accurate, which increases to 93% using the RIGHT operator (Woodcock and Gopal, 1994). The accuracy of the high resolution data is not particularly at issue, however, as this work focuses on changes in the cover type proportions as a function of resolution. While the 30-m class map may not perfectly represent the actual distribution of land-cover types at the surface, its composition and spatial characteristics can be considered representative of this type of landscape and, unlike the actual surface of an area of this size, its characteristics can be measured and known.

Description of Figures

The method outlined above was intended to allow the investigation of three primary questions. First, are the magnitudes of errors in land-cover proportions, which emerge as the scene is progressively aggregated, sufficiently large to be problematic at MODIS resolutions? Second, How strongly does the original size of classes affect the proportional error at coarser resolutions? Third, is such a class-size effect modified by the spatial characteristics of the component cover types? The results are displayed in several different ways in an attempt to provide insight into these issues.

Figure 1 shows the image proportions for the different cover types as the scene was aggregated to increasingly coarser scales. The space between the line for a given class

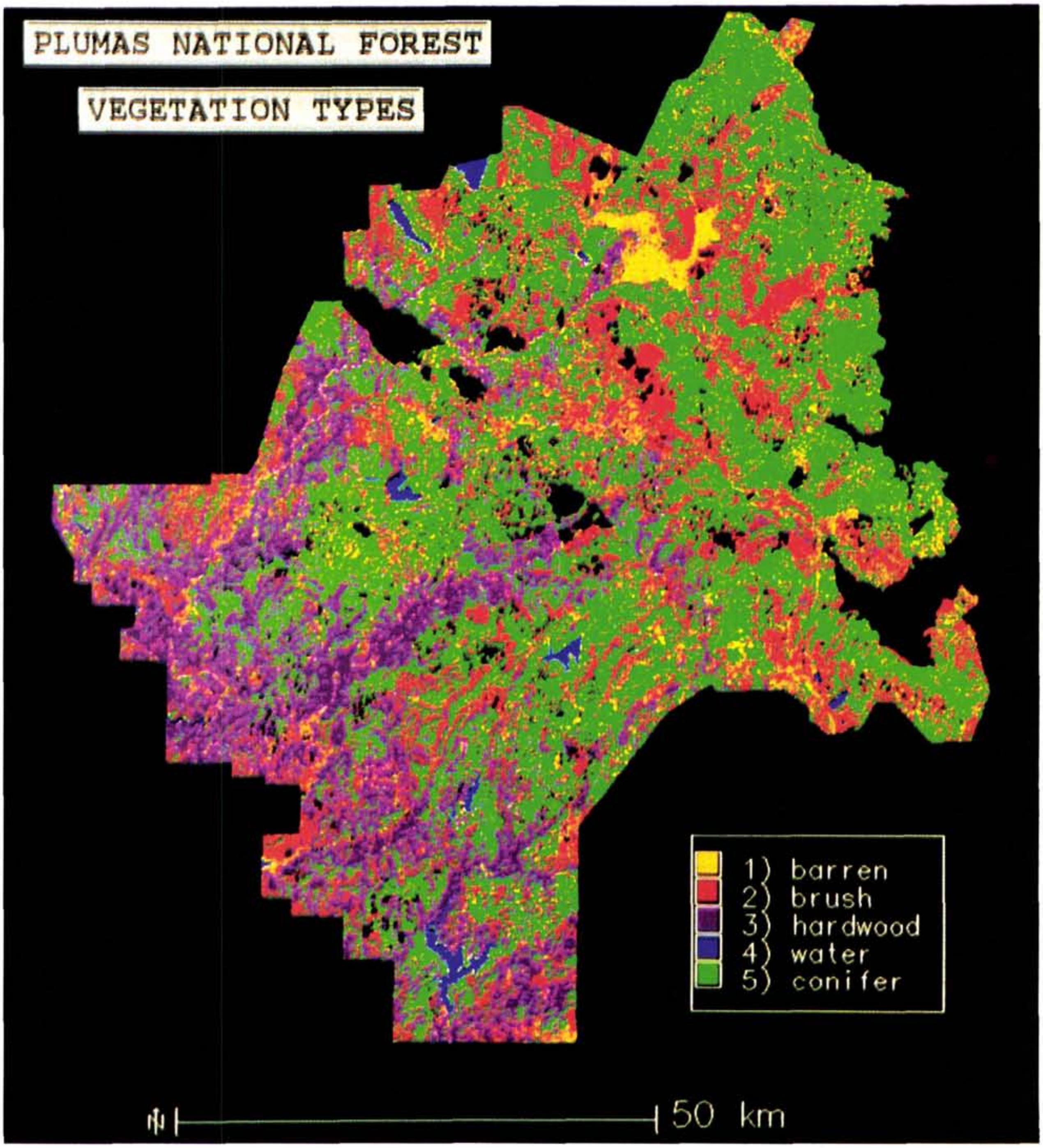

Plate 1. Plumas National Forest. Thirty-metre land-cover class map. red = *barren*, yellow = *brush*, purple = *hardwood*, green = *conifer*, blue = *water*, white = *other*. This represents the western two-thirds of the Plumas.

and the line below it represents the proportion of the image which is labeled as that class at a given resolution. Care must be taken in interpreting the slope of the lines as they are dependent upon the slopes of the lines below them.

Figure 2 shows proportional error as a function of resolution. The lines represent the proportion of the image added to or subtracted from the original proportion of each class for the different levels of aggregation. This can be thought of as the changes from the 30-m values in the distance between the lines in Figure 1. Figure 3 also shows proportional error

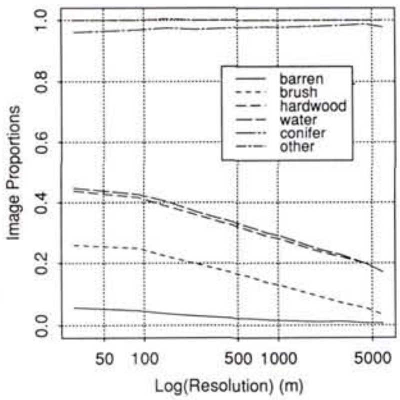

Figure 1. Changing proportions of different cover types as a function of aggregation level. The proportion of the image classified as a given cover type at a given resolution is represented by the distance between the line for the class of interest and the line below it.

with the *conifer* and *brush* classes removed so that *water, barren*, and *hardwood* can be observed more easily using an expanded scale on the *y*-axis.

While Figures 2 and 3 represent error relative to the entire image, they do not indicate the magnitude of the error relative to the original areal proportions of the individual classes. For example, while the proportion of *water* appears to have increased slightly at 150-m resolution, Figure 3 gives no indication of the percent by which *water* was overestimated. Figure 4 is similar to Figure 2 except that the values have been normalized by the areal proportions of each class at 30-m resolution. In this way we present an error graph which indicates the *percent* by which individual classes were over- or underestimated. It is cautioned that these error values are sensitive to the original size of a given class. For example *water*, which had a low initial image proportion, produced a large estimation error (Figure 4) while its proportional error (Figure 2) was quite low.

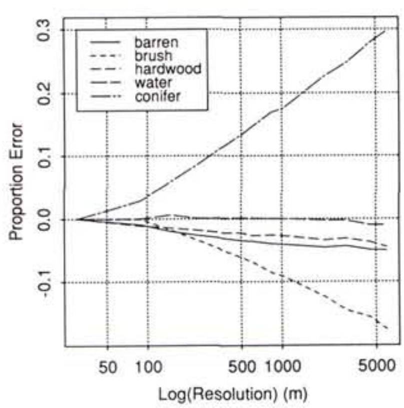

Figure 2. Proportional error as a function of resolution.

Figure 5 shows estimation error for each class at a sequence of resolutions. The cover types are ordered along the *x*-axis in terms of their relative image proportions in the original map; each line represents a different aggregation level. Note that the logarithm of resolution is used in these graphs as more detail exists in the data at the fine resolutions than at the coarser resolutions. The following discussion will refer to these figures. At this preliminary stage, only a qualitative assessment of the spatial nature of the different cover types in the scene is presented.

Results

Examination of Figure 1 shows the initial proportions of the different classes in the scene as well as their general response to progressive aggregation. At the original resolution, *conifer* is the dominant cover type, making up about 50 percent of the scene. *Brush* and *hardwood* are both moderately large classes, each comprising nearly 20 percent, with *barren* and *water* comprising about 5 percent and 1 percent of the original scene, respectively. The most apparent trends are that *conifer* exhibits very large positive proportional errors, and *brush* has large negative errors associated with scene aggregation. Because these were dominant classes initially, the large estimation errors are particularly significant in terms of adequately characterizing the relative proportion of cover types in the landscape. *Hardwood, water*, and *barren* decrease with resolution, but maintain relatively stable proportions throughout the aggregation sequence.

From Figure 1 and those that follow, it is clear that large errors arise due to aggregation. These errors may be unacceptable for many applications at the 1000-m resolution of the MODIS Land-Cover product. At 1020-m resolution, the proportion of the image labeled as *conifer* is increased by 17 percent of the entire scene, *brush* is decreased by 9 percent, and nearly 85 percent of the image is classified as either *conifer* or *hardwood*; an increase of 17 percent over the original resolution. As seen in Figure 4, these translate to a 34 percent overestimation for *conifer* and a 45 percent underestimation for *brush*. While the proportional errors for *water* and *barren* are fairly small, this is because these cover types comprise very little of the image at the original resolution. Both of these classes have high estimation errors as presented in Figure 4. If these classes were of interest to a user of the coarse resolution map — for example, due to their importance in surface/atmosphere interactions — these could present serious errors.

Figure 1 shows that all of the cover-type proportions remain fairly stable between 30- and 90-metre resolution. This suggests that 90 metres is finer than the fundamental scale of most of the smaller patches of the cover types in the scene, and that proportional accuracy can be maintained at this resolution for all classes. Beyond 90 metres, land-cover proportions change progressively with aggregation as the coarser resolutions are decreasingly adequate to resolve the landscape in terms of the cover types of interest. Figures 4 and 5 show perhaps more clearly the sharp break toward larger estimation errors at aggregation levels beyond 90 m. Notice in particular the very low errors for *brush* and *water* at 90 m, indicating that the typical patch size for these classes is such that this sampling resolution can accurately resolve the indi-

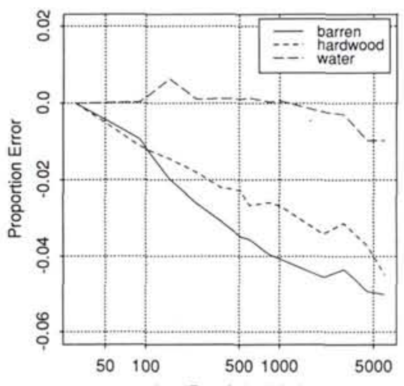

Figure 3. Proportional error as a function of resolution rescaled so that barren, hardwood, and water can be more easily interpreted.

vidual units. The low estimation error for all classes at 90 m suggests that, at this resolution, there is still a high degree of spatial autocorrelation in the scene as a whole. That is, any 30-m pixel, when observed at this scale, was more likely to be surrounded by its same class than by any other single cover type.

The large increase in error beyond 90 m indicates that spatial autocorrelation begins to break down at coarser scales. The smaller patches in the scene are not resolved by the coarser sampling grids, and, except for *conifer* and *water*, all class units are increasingly likely to be surrounded by some other individual cover type as aggregation proceeds. This implies that these cover types begin to occur in small, fragmented patches relative to the scale of observation at greater than 90-m resolution. While errors are generally low for all classes at 90 m, Figure 5 shows that *barren* has considerably greater estimation error than any other class at this resolution, and Figure 2 shows that *conifer* has much higher proportional error. These observations will be discussed in more detail below.

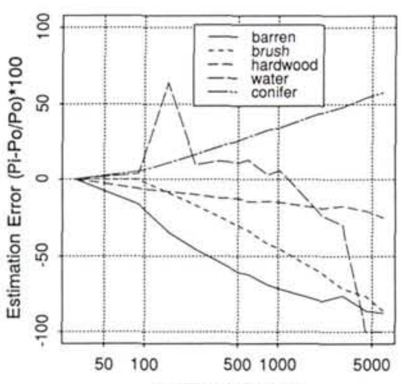

Figure 4. Estimation error as a function of resolution. This is the proportional error normalized by the proportions of the different classes at the original resolution to represent the percent by which individual classes were over or underestimated.

In general, Figure 5 suggests a trend in estimation error related to the original size of the classes. The smallest classes have large negative errors and the largest class has large positive errors. This appears to hold true with the exception of *water* and *hardwood*, which display anomalous behavior. The deviations from this trend suggest that scale-dependent estimation error is related not only to the actual proportions of the cover types in the scene, but also to the spatial characteristics of the component types.

Figure 5 illustrates a number of observations which can be explained by observable spatial patterns of the individual cover types. First, both the *barren* and *brush* classes steadily decrease in areal proportion until they nearly disappear at the coarsest resolution. Second, *hardwood* and *brush*, while making up roughly the same scene proportions initially, respond very differently to aggregation, with *hardwood* showing a very low estimation error overall, and *brush* rapidly diminishing toward large negative errors. Despite the low estimation errors for *hardwood* at most resolutions, this class has a relatively large negative error at 90 m. Third, the estimation error for *water* is extremely sensitive to aggregation resolution, ranging through small, large, and moderate overestimations and then falling off to moderate and then large underestimations. Finally, *conifer* is the only cover type to increase systematically throughout the entire range of aggregation scales.

Discussion

Images of the scene with each cover type displayed separately help explain the observed patterns in proportional errors by illustrating the spatial patterns of the classes. In Figures 6a through 6e, the grey areas fall outside the study area or represent unclassified pixels, white represents a single class, and all other classes are coded black.

While *barren* has the highest estimation error at 90 m, *brush* decreases much more rapidly than *barren* and, of all the classes, shows the greatest loss in areal proportion due to aggregation. Of the five classes, *barren* appears the most scattered and discontinuous except for one large homogeneous patch in the northern portion of the scene (Figure 6a). It is logical, therefore, that this class has the highest negative estimation error at 90-m resolution as its small units begin to be overwhelmed by other, more dominant cover types. *Barren* would probably disappear much more rapidly if not for the large barren area in the north. *Brush* (Figure 6b) maintains its correct image proportion at 90 m due to its slightly larger patch size and probably due to self-compensating gains and losses. However, because it is evenly scattered throughout the image, with very few closely spaced or large patches, it then begins to diminish rapidly and eventually attains extremely large negative errors.

The *hardwood* class is relatively insensitive to observation scale. At the initial resolution *hardwood* and *brush* have about the same areal proportion in the image. However, *hardwood* does not display the dramatic decrease in proportion that *brush* does. Rather, *hardwood* decreases gradually with aggregation and displays little loss in areal proportion, even at the coarsest resolution. Also, while *hardwood* is

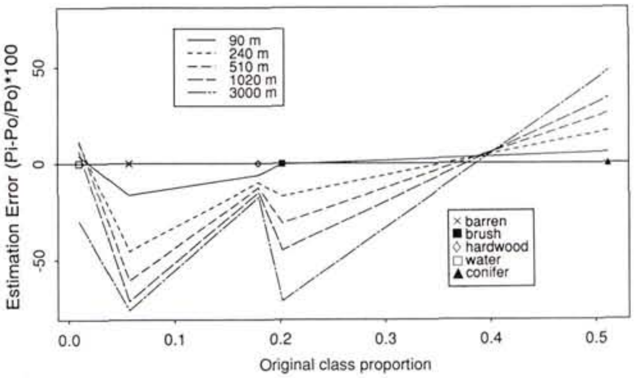

Figure 5. Estimation error as a function of original class proportion for five different aggregation levels.

clearly the most stable class overall, it has a high negative error relative to *brush* at 90 m while *brush* has much higher errors thereafter. Unlike *brush*, the *hardwood* pixels are concentrated in a limited portion of the entire area (Figure 6c). This pattern allows it to maintain its dominance in those areas at coarser resolutions. The fact that *hardwood* does not increase in proportion can be explained by its fragmented distribution in the eastern half of the site. The disappearance of these small scattered units probably leads to the relatively large negative error for this class at 90 m (Figure 4). It is likely that positive estimation error in the west is counteracted by negative error in the east, leading to the maintenance of high overall proportional accuracy for *hardwood*.

Only *water* displays a change in the direction of the estimation error. As the scene is aggregated, the proportion of *water* first increases up to a resolution of 150 m. Positive estimation errors then decrease until 1020 m when *water* begins to be underestimated, eventually disappearing entirely. While *water* covers only a small proportion of the original scene, this class exhibits high autocorrelation with moderately sized patches (Figure 6d). These patches are clearly large relative to the finer sampling resolutions, leading to the growth of the units and positive estimation errors between 90-m and 1020-m resolution. At 1020 m, *water* begins to be underestimated as the moderately sized patches become too small to be resolved and are overwhelmed by more common neighboring cover types (Figure 4).

Conifer has considerably larger proportional errors than any other class and is increasingly overestimated with progressive aggregation. The accumulation of small reductions in all of the other classes transfers to a relatively large increase in *conifer* at 90 m, and similarly at coarser scales. The *conifer* class exists throughout the scene and clearly dominates the landscape (Figure 6e). This class, therefore, rapidly grows in proportion as it is frequently the most common class against which smaller, more isolated patches are compared through the aggregation procedure.

Our results agree with the conclusions presented by Turner *et al.* (1989) that changes in cover-type proportions with the aggregation of spatial data are related to the scale of aggregation, the initial proportions of the component types, and the spatial arrangement of the landscape. While Turner *et al.* (1989) focused their analysis on over-all statistical measures for the entire scene, we have assessed our results in terms of observable spatial characteristics of the individual cover types. In actuality, it is probably a combination of cover-type-specific and scene-wide (interactive) spatial patterns which control the degree of proportional error with decreasing resolution. We have attempted to present this analysis with specific reference to remote sensing and, primarily, in the context of the implications for large-area land-cover characterization using coarse resolution satellite data.

Implications for Coarse-Scale Mapping

The results presented here have significant implications for land-cover mapping at coarse resolutions, such as those planned for MODIS. Given the limitations imposed by the fixed scale of observation, there appear to be two approaches available for handling the change in land-cover proportions resulting from a change in spatial resolution. First, the definition of land-cover classes can be adjusted to the physical reality that most resolution cells at a scale of 1 km are mixes of land covers. Land-cover classes at 1 km might be better defined explicitly as mixes of component land covers. This redefinition is easier to conceptualize for large classes which grow in areal proportion as resolution cell size increases, such as the conifer class in the Plumas data. However, the same explicit definition of proportions of land-cover types within land-cover classes would be necessary for all classes in a map. One way to estimate the component proportions of land covers within a class is to examine high-resolution maps like the 30-m Plumas land-cover map. Table 1 shows the proportions of land-cover types from the 30-m map found in the 1020-m map classes. It may be possible to calibrate these kinds of component mixes for land-cover classes for various ecoregions of the world. This approach would clearly involve a significant effort, and attention would have to be paid to the consistency with which these kinds of mixes could be calibrated in one location and used in neighboring areas. For further illustration, Figure 7 shows how the area mapped as *conifer* is actually partitioned among the five component cover types at a series of resolutions between 30 m and 1020 m. In this figure, the distance between the line for a given class and the line below it represents the proportion of the original map which is actually that class but has been re-classified as *conifer*. It would be valuable to test the stability of these relationships across similar regions.

A second approach would be to develop a method of estimating the original proportions of land covers in a scene from the proportions estimated from coarse resolution remotely sensed data. The exact form such a method might take is unclear at this point. One direction of future research will be to develop regression relationships that predict land-cover proportions at a coarse resolution as a function of the land-cover proportions at a fine resolution, the spatial properties of the fine resolution data, and the size of the coarse-resolution pixels. If these regressions are stable across locations and classes, the regression coefficients might be useful for estimating fine-resolution proportions from coarse-resolution estimates of land-cover proportions. A solution, or recommendation, for how to handle the issues associated with changing resolutions is beyond the scope of this paper, and will be pursued in future work. The data presented here are primarily helpful in the context of illustrating the nature and magnitude of the problems to be encountered.

Conclusions

Significant proportional errors arise as land-cover data are sampled at progressively coarser scales. These errors can be

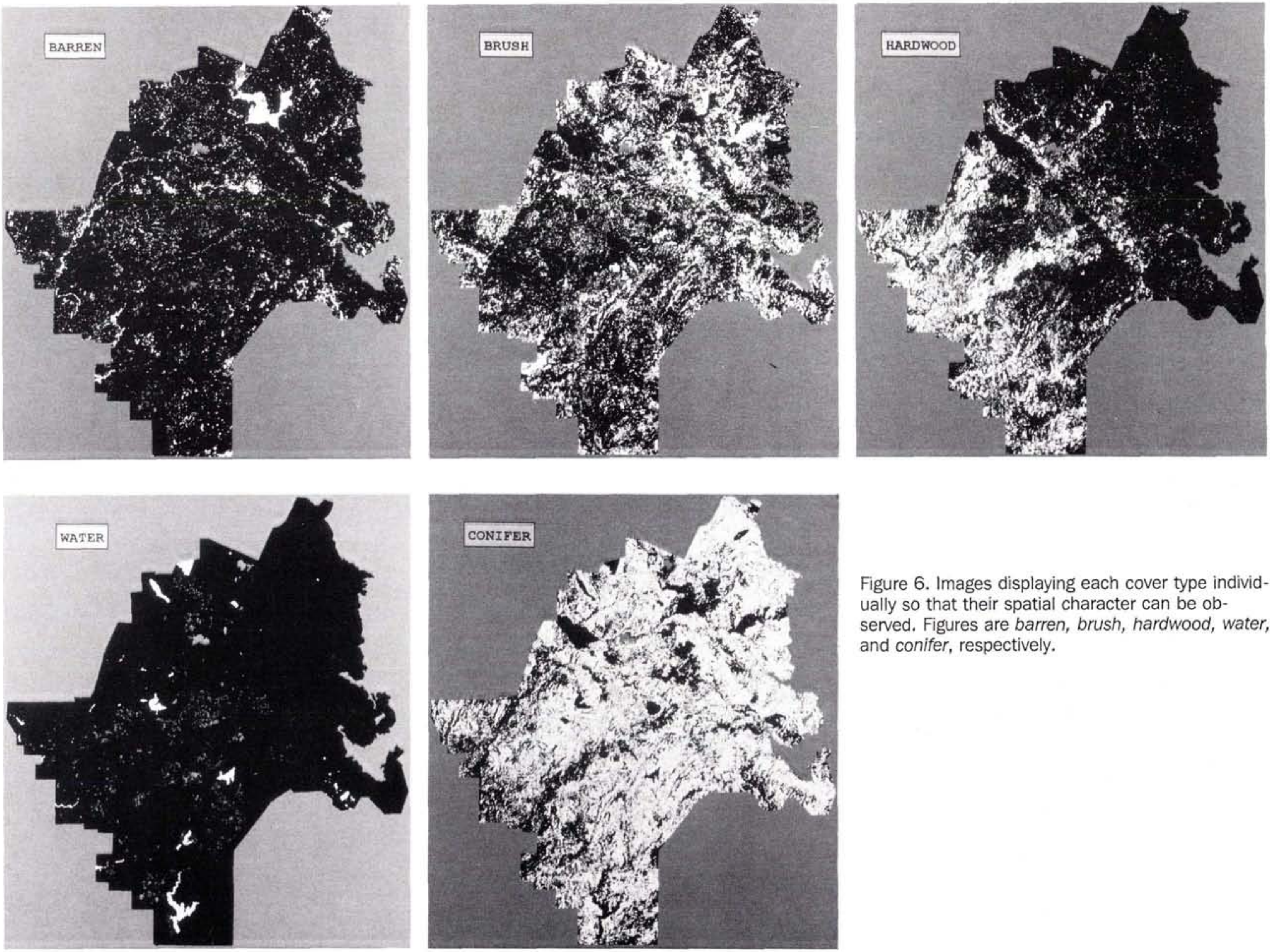

Figure 6. Images displaying each cover type individually so that their spatial character can be observed. Figures are *barren*, *brush*, *hardwood*, *water*, and *conifer*, respectively.

Table 1. Proportion of each Cover Type in the 1020 m Aggregated Class Map Which Was Classified as Each Component Type at the Initial Resolution.

Composition of Land-Cover Classes at 1020 Meters						
	Aggregated Cover Type					
Components	barren	brush	hardwood	water	conifer	other
barren	0.644	0.118	0.040	0.068	0.039	0.033
brush	0.196	0.491	0.154	0.060	0.174	0.086
hardwood	0.053	0.122	0.520	0.047	0.127	0.040
water	0.007	0.003	0.004	0.645	0.003	0.000
conifer	0.092	0.245	0.277	0.179	0.643	0.140
other	0.007	0.022	0.004	0.001	0.013	0.701

of sufficient magnitude to compromise the utility of land-cover maps produced using coarse-resolution remotely sensed data such as that provided by NOAA-AVHRR or the future MODIS sensor. Although formal analysis of the affect of spatial pattern on scale-dependent proportional error was not conducted at this stage, several general observations have emerged. Classes consisting of large, homogeneous patches, such as *conifer*, grew larger as the sampling resolution was degraded. While such classes may not always represent a majority of the pixels in a sampling unit, they tend to be the most common cover type, especially near their patch boundaries when the other component types are distributed in small, fragmented units. This will cause their boundaries to expand as the scene is sampled at increasingly coarser scales. Classes characterized by highly clumped distributions, but small or intermediate sized patches (such as *water*), first grow (as above), and then decrease in size as the sampling resolution is progressively degraded beyond the typical patch size for that class. Classes composed of small, fragmented units rapidly disappear as they are dominated by more clumped cover types through the aggregation procedure. Naturally, most classes do not fall neatly into any of these categories. The error for most classes results, therefore, from some combination of the responses to aggregation suggested above.

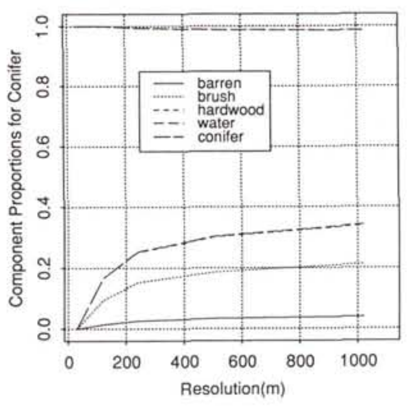

Figure 7. Changing proportions of component cover types contributing to the *conifer* class as reclassified at a range of resolutions through aggregation.

This work represents a qualitative investigation into the existence and systematic nature of the relationship between scene spatial characteristics and the magnitude, direction, and scale dependence of proportion estimation errors. Future work will focus on a quantitative analysis of these relationships and attempt to establish a basis for the development of scaling transfer relationships for proportional error associated with coarse-scale characterization of land-cover data.

Acknowledgment

This work was supported by the National Aeronautics and Space Administration under contract NAS5-31369. The authors gratefully acknowledge John Collins, Vida Jakabhazy, Scott Macomber, and Soren Ryherd for their work in producing the Plumas land cover classification; and Jud Harward for improvements in the processing algorithm.

References

Cushnie, J. L., 1987. The interactive effect of spatial resolution and degree of internal variability within land-cover types on classification accuracies, *Int. J. Remote Sens.*, 8(1):15–29.

Davis, F. W., D. A. Quattrochi, M. K. Ridd, N. S-N. Lam, S. J. Walsh, J. C. Michaelsen, J. Franklin, D. A. Stow, C. J. Johannsen, and C. A. Johnston, 1991. Environmental analysis using integrated GIS and remotely sensed data: Some research needs and priorities, *Photogrammetric Engineering & Remote Sensing*, 57(6):689–697.

Gervin, J., A. Kerber, R. Witt, Y. Lu, and R. Sekhon, 1985. Comparison of level I land cover classification accuracy for MSS and AVHRR data, *Int. J. Remote Sens.*, 6(1):47–57.

Gopal, S., and C. E. Woodcock, 1994. Theory and methods for accuracy assessment of thematic maps using fuzzy sets, *Photogrammetric Engineering & Remote Sensing*, 60(02):181–188.

Hobbs, R. J., 1990. Remote sensing of spatial and temporal dynamics of vegetation, *Remote Sensing of Biosphere Functioning* (R. J. Hobbs and H. A. Mooney, editors), Springer-Verlag, New York.

Latty, R. S., and R. M. Hoffer, 1981. Computer-based classification accuracy due to the spatial resolution using per- point versus per-field classification techniques, *Machine Processing of Remotely Sensed Data Symposium*, West Lafayette, Indiana, pp. 384–392.

Loveland, T. R., J. W. Merchant, D. O. Ohlen, and J. F. Brown, 1991. Development of a Land-Cover Characteristics Database for the Conterminous U.S., *Photogrammetric Engineering & Remote Sensing*, 57:1453–1463.

Markham, B. L., and J. R. G. Townshend, 1981. Land cover classification accuracy as a function of sensor spatial resolution, *Proc. of the 15th Int. Symp. on Remote Sensing of Environment*, Ann Arbor, Michigan, pp. 1075–1090.

Matthews, E., 1983. Global vegetation and land use: New high resolution data bases for climate studies, *J. of Appl. Meteor*, 22:474–487.

Meentmeyer, V., and E. Box, 1987. Scale effects in landscape studies, *Landscape Heterogeneity and Disturbance* (M. Turner, editor), Springer-Verlag, New York, pp. 15–34.

Olson, J. S., and J. A. Watts, 1982. *Major World Ecosystem Complexes*, Oak Ridge National Lab, Oak Ridge, Tennessee.

Rosen, R., 1989. Similitude, similarity, and scaling, *Landscape Ecology*, 3:207–216.

Running, S., C. Justice, D. Hall, A. Huete, Y. Kaufman, J. Muller, A. Strahler, V. Vanderbilt, Z. Wan, P. Teillet, and D. Carneggie (submitted). Terrestrial remote sensing science and algorithms planned for EOS/MODIS, *Int. J. Remote Sensing*.

Sadowski, F. G., J. E. Malila, J. E. Sarno, and R. G. Nalepka, 1977.

The influence of multispectral scanner spatial resolution on forest feature classification, *Proc. of the 11th Int. Symp. on Remote Sensing of Environment*, Ann Arbor, Michigan, pp. 1279–1288.

Townshend, J., and C. Justice, 1988. Selecting the spatial resolution of satellite sensors required for global monitoring of land transformations, *Int. J. Remote Sensing*, 9(2):187-236.

———, 1990. The spatial variation of vegetation changes at very coarse scales, *Int. J. Remote Sensing*, 11(1):149–157.

Townshend, J., C. Justice, W. Li, C. Gurney, and J. McManus, 1991. Global land cover classification by remote sensing: Present capabilities and future possibilities, *Remote Sens. Environ.*, 35:243–255.

Townshend, J. R. G., C. O. Justice, and V. Kalb, 1987. Characterization and classification of South American land-cover types using satellite data, *Int. J. Remote Sensing*, 8:1189–1207.

Tucker, C. J., J. R. G. Townshend, and T. E. Goff, 1985b. African land cover classification using satellite data, *Science*, 227:369–375.

Turner, M., R. O'Neill, R. Gardner, and B. Milne, 1989a. Effects of changing spatial scale on the analysis of landscape pattern, *Landscape Ecology*, 3(3/4):153–162.

Turner, M., V. Dale, and R. Gardner, 1989b. Predicting across scales: Theory development and testing, *Landscape Ecology*, 3(3/4):245–252.

Turner, S., R. O'Neill, W. Conley, M. Conley, and H. Humphries, 1991. Pattern and scale: Statistics for landscape ecology, *Quantitative Methods in Landscape Ecology: The Analysis and Interpretation of Landscape Heterogeneity* (M. Turner and R. Gardner, editors), Springer-Verlag, New York.

Wilson, M., and A. Henderson-Sellers, 1985. A global archive of land cover and soils data for use in general circulation climate models, *J. Climatol.*, 5:119–143.

Woodcock, C. E., and A. H. Strahler, 1987. The factor of scale in remote sensing, *Remote Sens. Environ.*, 21:311–332.

Woodcock, C. E., J. Collins, S. Gopal, V. Jakabhazy, X. Li, S. Macomber, S. Ryherd, Y. Wu, V. J. Harward, J. Levitan, and R. Warbington, 1993. Mapping forest vegetation using Landsat TM imagery and a canopy reflectance model, submitted to *Remote Sens. Environ.*, June, 1993.

———, 1994. Accuracy assessment of the Plumas National Forest Vegetation Map, in preparation for *Photogrammetric Engineering & Remote Sensing*.